MagTouch: Robust Finger Identification for a Smartwatch Using a Magnet Ring and a Built-in Magnetometer

Keunwoo Park[1], Daehwa Kim[1], Seongkook Heo[2], and Geehyuk Lee[1]
[1]HCI Lab, School of Computing, KAIST, Daejeon, Republic of Korea
[2]Department of Computer Science, University of Virginia, Charlottesville, Virginia, United States
{keunwoo, daehwakim}@kaist.ac.kr, seongkook@virginia.edu, geehyuk@gmail.com

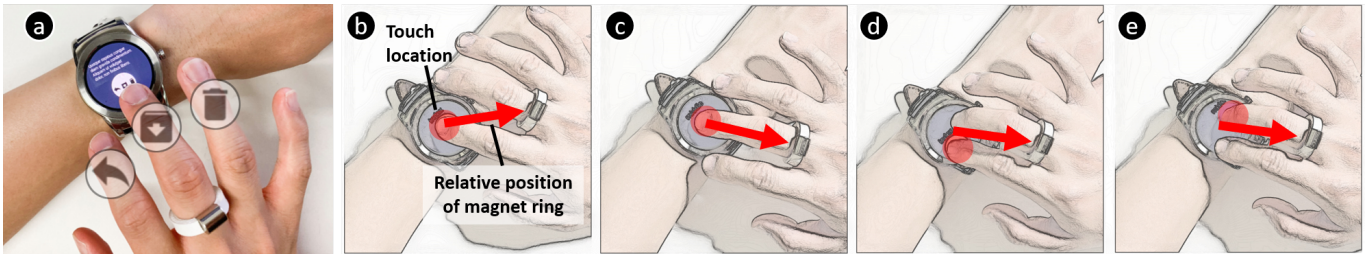

Figure 1. MagTouch identifies the contact finger among index, middle, and ring fingers using an embedded magnetometer in a smartwatch and a permanent magnet ring. (a) A user can invoke three different functions on a single button by simply switching between fingers. Based on the touch location and the magnetic field vector, MagTouch can identify the contact finger when a user moves the hand to switch between fingers (b,c) and when the user only switches the contact fingers without moving the hand (d,e).

ABSTRACT
Completing tasks on smartwatches often requires multiple gestures due to the small size of the touchscreens and the lack of sufficient number of touch controls that are easily accessible with a finger. We propose to increase the number of functions that can be triggered with the touch gesture by enabling a smartwatch to identify which finger is being used. We developed MagTouch, a method that uses a magnetometer embedded in an off-the-shelf smartwatch. It measures the magnetic field of a magnet fixed to a ring worn on the middle finger. By combining the measured magnetic field and the touch location on the screen, MagTouch recognizes which finger is being used. The tests demonstrated that MagTouch can differentiate among the three fingers used to make contacts at a success rate of 95.03%.

Author Keywords
Touch, Finger Identification, Magnetic, Smartwatch

INTRODUCTION
Smartwatches allow users to access information and notifications at a glance[40]. They are significantly faster to access than smartphones [3] and allow for microinteractions, which takes less than few seconds [2] and do not slow down secondary tasks in mobile scenarios [37]. However, efficient input on smartwatches is still challenging, especially with touch buttons [40]. As the number of graphical user interface (GUI) controls on the screen is limited because of its size, completing a simple task often requires a series of swipe and tap gestures that may extend task completion times, result in fatigue, and hinder the completion of secondary tasks [37]. Speech input is supported by many smartwatches and can be helpful with complex commands, however, it may not be practical in some public setting due to the social acceptability [41] and noise concerns.

We believe that expanding the touch input vocabulary without increasing the density of touch controls on smartwatches will assist users to complete tasks more rapidly on their smartwatches and focus on their primary tasks. One approach to achieving this objective is by identifying the fingers and, thereby, diversifying input operations, as in practice, people use each finger differently. For example, when using a computer mouse, index and middle finger are dedicated to different buttons, which leads to various functions being activated. Similarly in a smartwatch, tapping on the same button may open an item (index finger), open a context menu (middle finger), or trigger an alternative function (Figure 1a). Finger identification has produced numerous beneficial results across many digital devices, from tabletops [5, 7, 22, 35] to mobile phones [4, 12, 17], and smartwatches [15, 18]. This is achieved using computer-vision based techniques [13, 44, 47, 50], finger-worn sensors and actuators [18, 31], or using other body-worn sensors such as electromyography electrodes [7]. Although the abovementioned studies have demonstrated the potential benefits of employing finger identification methods, however, these methods are not feasible for smartwatches [5, 30, 50]. Requirements such as active sensing/actuation elements attached to fingers [31], can interfere with people's

CHI '20, April 25–30, 2020, Honolulu, HI, USA.

ACM ISBN 978-1-4503-6708-0/20/04 ...$15.00.
http://dx.doi.org/10.1145/3313831.3376234

daily activities when using their hands and make them hesitant of wearing such devices because of aesthetics [32].

Our objective was to create a practical and robust method to enable finger-identification on a smartwatch with minimal effect on the wearer's appearance or hand-based activities. This paper presents *MagTouch*, a method that uses a magnetometer embedded in a smartwatch and a magnet ring to identify the three operating fingers (See Figure 1). It uses both magnetometer data and touch locations for identification. This is not the first work to use a magnet in smartwatch interactions as researchers have previously investigated the use of a magnet on a fingertip or fingernail [9, 20, 33]. We focused on developing a more practical solution that causes minimal inconvenience for everyday wear and decided to use a ring for that purpose. Placing a magnet distant from the smartwatch creates several challenges. Interference from ambient magnetic fields (e.g., a geomagnetic field) increases due to the attenuation of the magnetic field of the magnet ring. The ambiguity in identifying the fingers also increases because, unlike with other magnet tracking systems, the smartwatch uses a single magnetometer [9, 33].

In this paper, we describe the methods implemented to cope with the challenges, including an algorithm that compensates for the ambient magnetic field and the combined use of magnetic field and touch location. To validate this concept, we devised a prototype with a conventional smartwatch and a ring with a magnet. Our evaluation showed that MagTouch could successfully identify the fingers over 95% of the trials with different orientations and usage contexts where the ambient magnetic field could change dynamically. This result is an improvement of 22% over the method that uses magnetic field measurement without dynamic calibration (77.9%) [38].

In summary, our work contributes a practical and robust finger identification method that uses a magnet ring and a built-in magnetometer. Furthermore, we offered the project resources online for researchers to use finger identification in their work (https://github.com/KAIST-HCIL/MagTouch).

RELATED WORK

Finger Identification Techniques

Researchers sought ways to detect the finger touching the screen and developed interaction techniques that utilize finger identification to enrich touch interaction.

Computer vision is the most common method of finger identification. Colley et al. [12] proposed a contact list application where different actions were mapped to the five fingers. They utilized a leap motion to determine which finger was interacting with the smartphone. Zheng and Vogel [50] designed a finger identifying keyboard for shortcuts. The same key could map to a regular key input or a shortcut, depending on which finger was used to press the key. They used a hand image and a $1 Recognizer to identify which finger was pressing which key. Sridhar et al. [44] proposed a music player that could be controlled with the thumb and the index finger. When a user touched the back of a hand with her index finger the volume increases and touching it with the thumb the volume decreases. Depth sensor on a user's arm distinguished which fingers touched the back of the user's hand.

Researchers have developed other approaches that do not use a camera. Dualkey [18] used a finger-worn optical sensor to identify fingers (i.e. sensor-worn finger vs. naive finger) and showed that it could increase typing speed on a smartwatch by mapping two characters to a single key. Gupta et al. [17] demonstrated using the same sensor that having two touch modes could enable seamless application switching on a smartphone. Benko et al. [7] used electromyography signals measured from the forearm and demonstrated the use of finger identification by presenting a painting application that allowed a user to draw with different colors with different fingers. Gil et al. [15] developed TriTap that uses a raw capacitance image obtained from a touchscreen to distinguish between thumb, index, and middle fingers. Instead of using finger identification itself, researchers also explored more sophisticated uses such as a multi-function touch buttons [42] and finger-specific chord gestures [5, 46].

While several finger identification technologies exist, a practical technology for a smartwatch is still required. Computer-vision based technologies [12, 13, 16, 29, 30, 35, 44, 47, 50] are difficult to use for smartwatches because of the viewing angle of a camera. A camera and a hand should be distanced and this limitation is critical for designing a wearable device. Finger-worn sensors [17, 18, 31] and arm-worn sensors [7] can be cumbersome for daily activities, and fingerprints [22, 45] are unavailable for smartwatches. TriTap [15] can identify fingers without additional sensors; however, a user needs to exaggerate her posture to achieve high accuracy.

Using Magnetic Field Sensing for Interaction

Many studies used magnets to interact with mobile and wearable devices as they do not require any power sources to generate a magnetic field and are therefore, comfortably mobile.

One of the most common locations for magnet placement is the fingertip [9, 10, 19, 20, 33]. By using a dual-axis magnetic sensor [20] or using multiple magnetic sensors [9, 10, 19, 33] researchers demonstrated that the magnets attached to the fingertip can enable in-air gestures [20, 33] and 3D input [9, 10] on mobiles. Chen et al. showed that using electromagnets that oscillate at certain frequencies can enable tracking of multiple magnets [10] and eliminates the effect of a geomagnetic field.

Some systems used a magnet ring. With Nenya [1], users could control a circular UI by rotating a ring with a magnet worn on a finger. Ketabdar et al. [24] used an embedded magnetic field sensor to enable around-device gestures made with a finger wearing magnet ring, for a smartwatch. While Cheung and Girouard [11] also used a magnet ring but the ring was used while held in hand as a tangible interface, instead of being worn.

Researchers also investigated the use of magnets for enriching touch interaction. GaussBits [26] recognized an object on a screen with a magnetic sensor grid and showed visual information related to the object. A user could change the input modes of a smartphone using MagNail [23] by attaching a

magnet to a user's nail. Ates et al. [4] attached a magnet to a fingertip and used the polarity of the magnetic field to expand touch gestures. TRing [49] is a technology that estimates orientation and the position of an inertial measurement unit (IMU) sensor relative to a magnet.

While there was no study that investigated the use of a finger-worn magnet ring for enriching touch interaction, Park et al. [38] reported preliminary study results on using a magnet ring for finger identification with early guidelines for designing a magnet ring. As it was an early investigation of the method, we advanced the objective by improving the algorithm to be less sensitive to magnetic fields in the environment and evaluated its performance characteristics in practical settings.

Summary

Limited input vocabulary has been a well-known problem in the field of HCI, and many methods have been developed to cope with it. While these methods demonstrate significant improvements, most techniques are difficult to implement in everyday devices due to wearability challenges [7, 9, 10, 18, 19, 20, 33] or the difficulties of employing the technology for smartwatches [22, 45]. This paper presents a practical solution by using a magnet ring and an off-the-shelf smartwatch. We present the challenges coming from the use of the ring and their solutions.

MAGTOUCH: FINGER IDENTIFICATION USING MAGNET RING

When a hand wearing a magnet ring touches a smartwatch, the magnetic field and the touch location are determined by the contact finger, as illustrated in Figure 1. It shows a user wearing a smartwatch on the left hand and a magnet ring on the middle finger of the right hand touching the screen. The positions of each fingertip relative to the center of the hand do not change when touching a surface. Therefore, it is possible to identify the touching finger from the touch location and the position of the center of the hand. For example, if the touch point is at the left side of the right hand, then the contact was made with the index finger. We attached a magnet to a hand to get information about the hand's location using the magnetometer. Figure 1b-c illustrates that the relative position of the magnet ring shifts when a user touches the smartwatch with a different finger. This leads to changes in the magnetic field vector at the smartwatch's magnetometer. Alone, magnetic field data is not sufficient for our purposes. Magnetic field data can be replicated by different contact fingers, as Figure 1d-e, unless the touching hand moves. For such cases, touch location data is used to identify the fingers accurately. Figure 2 shows ambiguity when only the magnetic field data is used.

There are many possible ways to attach a magnet to a hand. Attaching a magnet to a fingertip and wearing a magnet ring were the most popular approaches. We selected the ring because its shape is suitable for everyday activity. It is mechanically challenging to fix a magnet to a curvilinear surface when we take account daily activities such as washing hands and typing

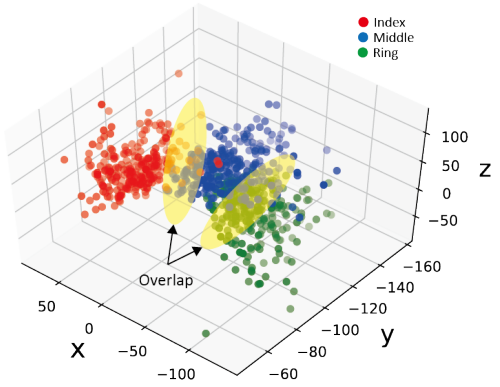

Figure 2. Magnetic field data when touching various locations of the smartwatch's touchscreen. Magnetic field can be similar even if a touching finger is different. Touch location data is necessary for such cases.

keyboards. Furthermore, rigid object attached directly on the skin might cause irritation and discomfort [27].

Rings are usually worn near the metacarpophalangeal joint of a finger. Transferring a fingertip-magnet to a ring poses a challenge related to the ambient magnetic field. MagTouch cannot avoid measuring the ambient magnetic field, even though it should only measure the magnetic field from a magnet ring. The ambient magnetic field can be considered noise and the noise becomes more significant when a magnet is on a ring rather than a fingertip. As the distance between the magnet and the smartwatch (r) increases, the magnetic field of the magnet decreases by the cube of the distance, and the relative portion of the ambient magnetic field ($\mathbf{B}_a$) increases. This relationship can be described as using the following equation:

$$\mathbf{B}_m = \frac{\mu_0}{4\pi}\left[\frac{3\hat{\mathbf{r}}(\mathbf{m}\cdot\hat{\mathbf{r}})-\mathbf{m}}{r^3}\right]+\mathbf{B}_a \quad (1)$$

$\mathbf{B}_m$ refers to the magnetic field vector at a point. $\mathbf{m}$ is magnetic moment of a magnet. $\hat{\mathbf{r}}$ denotes the direction of the point from the magnet. To compensate for magnetic field degradation over distance substantially stronger magnet is needed. However, as a wearable solution it is impractical, as a stronger magnet is usually larger.

A simple pilot test was conducted to compare the magnitude of a fingertip magnet and a magnet ring relative to the ambient magnetic field. The test required a person to touch the smartwatch with their middle finger. A magnet ($\phi 6 \times 5\,\text{mm}$) was fixed to nail of the middle finger and the first joint of the middle finger. The person rotated 180° while touching a point on the smartwatch. The magnetic field magnitude changed when the person rotated, because the direction of the ambient magnetic field relative to the watch was changed. If the change is large, the portion of the ambient magnetic field is large. As shown in Figure 3, the difference of magnetic field magnitudes was more significant when the magnet was far from the smartwatch (*magnet on nail vs. magnet on ring*). As a magnet moves away from the smartwatch, the ambient magnetic field noise increased. A double sized magnet ($\phi 7.5 \times 9.5\,\text{mm}$) was tried, but the ambient magnetic field still intruded.

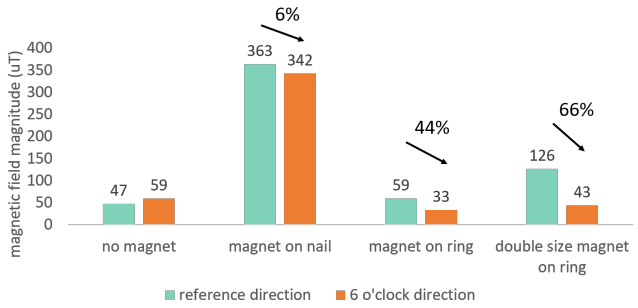

Figure 3. Change in the magnitude of magnetometer vector data with the change in the ambient magnetic field. The magnetometer vector data is a vector sum of the magnetic field of the magnet ring and the ambient magnetic field. The reference and 6'o clock directions denotes two opposite directions.

It is necessary to examine the physical model underlying MagTouch to understand the challenges, including the ambient magnetic field problem facing the development of a practical system. The magnetic field measured by the internal magnetometer of the smartwatch is the sum of the magnetic field from the magnet ring and the ambient magnetic field. The magnetic field from the magnet ring is determined by the position and the orientation of the ring relative to the smartwatch. This in turn depends on three main variables: which finger touches the screen, the contact point on the screen, and the relative orientation of the right hand to the left hand. Figure 4a graphically illustrates these dependencies. The goal of MagTouch is to infer which finger is touching the screen from only the touch location and the magnetic field measured by the smartwatch magnetometer. This is a challenging inverse problem because of two unknown variables: the ambient magnetic field and the relative orientation of the right hand. Park et al. [38] showed that this inverse problem could be solved when the two variables are predefined.

The MagTouch method handles the first unknown variable using a sub-module called *Computational Ambient Magnetic field Eliminator* (CAME). CAME measures and saves the ambient magnetic field when the magnet ring is at distance from the smartwatch, i.e., when the magnetic field from the ring is negligible. When the magnet ring approaches, the magnetic field around the smartwatch distorts. CAME detects the distortion and subtracts the recorded ambient magnetic field from the magnetic field, measurement leaving only the magnetic field of the magnet ring.

After the first unknown variable is removed, selecting from the three fingers may be possible in the presence of the second unknown variable. In this study, we show that the MagTouch method accurately identifies the touching finger when the posture of the ringed hand is within normal use range. Figure 4b conceptually depicts the computations executed by the MagTouch method. The effect of the ambient magnetic field is removed first. MagTouch then identifies the contact finger based on the magnetic field by the magnet ring and the touch position using a machine learning model which is trained with data collected in various hand postures. Our results showed

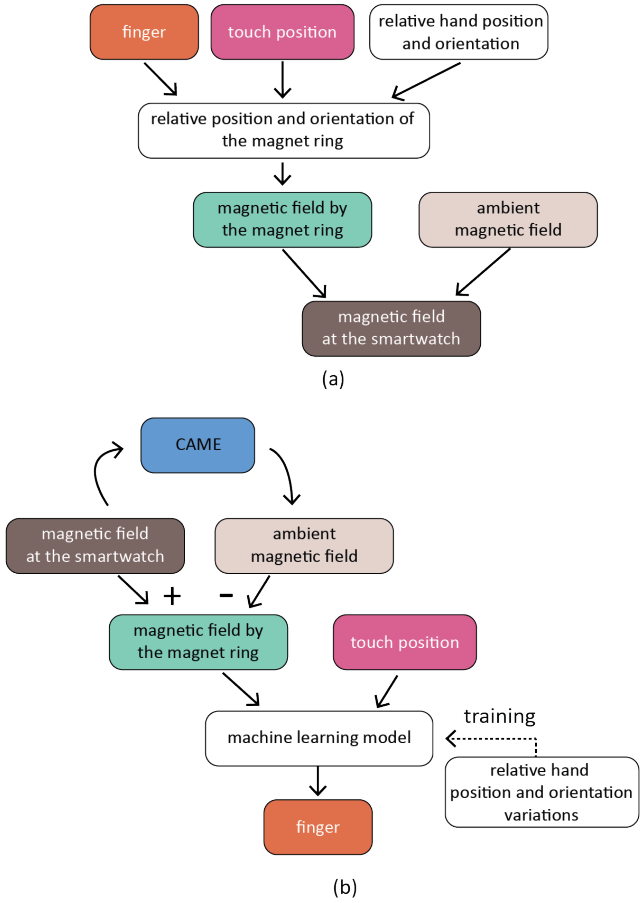

Figure 4. The MagTouch method: (a) physical model and (b) the inverse problem for finger identification.

that the classifier margins of the resultant machine learning model could successfully accommodate the variation of relative hand positions and orientations occurring during normal smartwatch use.

Hardware Implementation

MagTouch can be implemented using a smartwatch equipped with a 9 degrees of freedom IMU (accelerometer, gyroscope, and magnetometer) and a ring with a permanent magnet. Figure 5 shows our implementation of MagTouch that used an unmodified LG Urbane smartwatch. As the permanent magnet is the only essential component of the ring, it can be made in different shapes using different materials (See Figure 5b, c).

The magnet's orientation was decided based on the simulation by Park et al. [38], which showed that the best finger identification results were found when placing the magnet perpendicular to the finger. We selected a magnet with a magnetic field reaching up to 100 mm. This is presumably longer than most middle fingers [6, 36, 39], and the magnetic field can be detected by a sensor on the opposing wrist. The cylindrical ($\phi 7.5 \times 9.5$ mm) magnet's magnetic field was 18 µT measured at the perpendicular distance of 100 mm from its axis.

In our experiments, as seen in Figure 5d, we used a ring fabricated of a rubber band to accommodate different finger sizes and used a 3D-printed spacer lodged between the smartwatch and the wrist to secure it for participants whose wrists were too small for the shortest watch band setting.

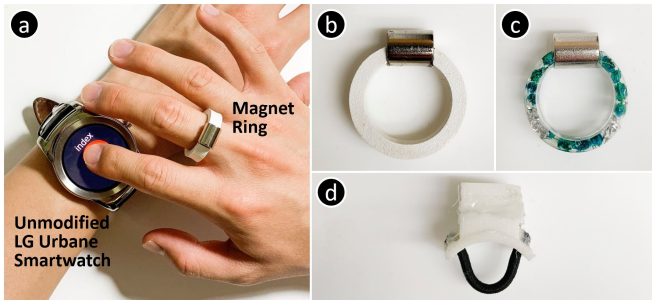

Figure 5. MagTouch hardware implementation. a) Smartwatch and magnet ring worn in hands. Magnet rings made with b) ABS plastic and c) resin. d) Magnet ring with rubber band used for experiments.

Software Implementation

MagTouch software consists of two parts, as shown in Figure 6. The first part, which we call CAME, estimates the magnetic field of the magnet ring. The second part is a machine learning classifier, which predicts a touching finger with a touch location and a magnetic field vector measured at the sensor.

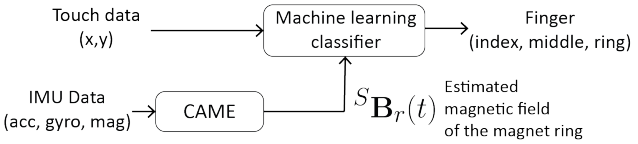

Figure 6. MagTouch system overview.

CAME measures the magnetic field of the magnet ring by subtracting the ambient magnetic field from the magnetometer data. This is critical to the process because the ambient magnetic field can be a source of errors. Even though a user touches the same location on the smartwatch with the same finger, the magnetic field measurement changes according to the smartwatch's orientation relative to the earth. This section explains the details of CAME and the classifier.

Computational Ambient Magnetic Field Eliminator (CAME)

The concept of CAME is explained as follows; when the magnet ring is not nearby, the ambient magnetic field is measured and stored. When the magnet ring approaches the magnetic field around the smartwatch, distorts the magnetic field. Subsequently, CAME subtracts the saved ambient magnetic field data from the measured magnetic field. As a result, only the magnetic field of the magnet ring remains. The concept is simple, but requires elaborate computation because the watch may move and rotate during the ambient magnetic field subtraction process.

CAME uses the attitude and heading reference system (AHRS) by Madgwick et al. [28] to find correct direction of the ambient magnetic field. The AHRS utilizes an accelerometer, a gyroscope, and a magnetometer to estimate the orientation of an IMU sensor. The gyroscope data is used for calculating the rotated angle; however it is prone to drift errors. As a solution, the AHRS optimizes the orientation of an IMU sensor to minimize the difference between measured and true values of gravity and the earth's magnetic field. Once the AHRS finds a stable orientation, the magnetometer is not required for some time, because the accelerometer can handle some of the drift error by itself. The accuracy of measurements with and without a magnetometer were close in Madgwick et al. [28]'s paper. CAME uses this knowledge to estimate orientation of the ambient magnetic field when the magnet ring is near the smartwatch.

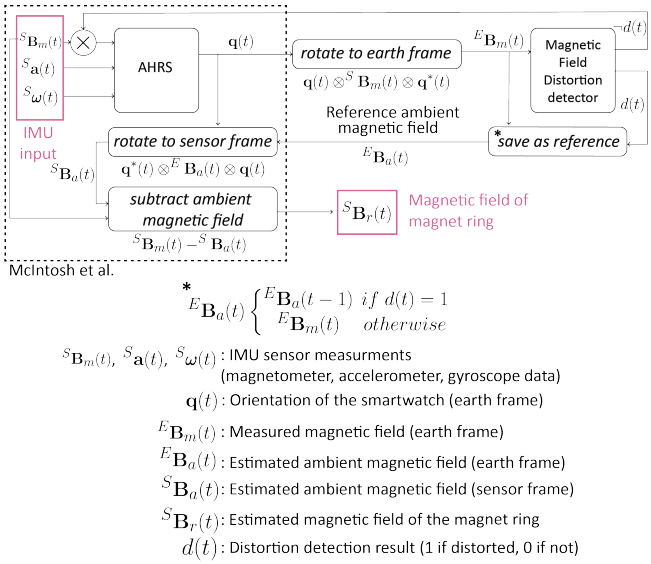

Figure 7. Overview of the CAME method.

As illustrated in Figure 7, CAME estimates the orientation of the smartwatch with all three sensors when the magnet ring is not near. In addition, it continuously rotates the magnetic field data to the earth's frame, and saves it as the reference ambient magnetic field ($^{E}\mathbf{B}_a(t)$). When the magnet ring approaches, CAME stops saving the magnetic field data, and uses the saved magnetic field data as the $^{E}\mathbf{B}_a(t)$. CAME rotates the $^{E}\mathbf{B}_a(t)$ to change its frame from the earth frame to the sensor frame ($^{S}\mathbf{B}_a(t)$). Now, the $^{S}\mathbf{B}_a(t)$ is the estimated ambient magnetic field to the sensor frame. CAME subtracts the $^{S}\mathbf{B}_a(t)$ from the magnetometer data to get the magnetic field of the magnet ring.

A similar method was initially proposed by McIntosh et al. [33] and it was named "geomagnetism cancellation." However, the two approaches differ in detail. McIntosh et al. assumed a constant ambient magnetic field. We considered wearable environments where a user could be moving between locations. In such cases, the ambient magnetic field can change even in the same building [43] due to ferromagnetic materials (e.g. steel) in walls or other objects. Therefore, MagTouch continuously updates the reference ambient magnetic field. Moreover, the magnet detection methods are different. The

existence of the magnet ring is detected by the *magnetic field distortion detector* and it is an important block of CAME. The detection procedure is explained in the next subsection.

CAME requires an initialization step. The AHRS takes time to converge and find the sensor's orientation. We set the initialization time to 20 s which, depending on the parameters of AHRS, is longer than the required. Usually, a few seconds are enough to ensure that it is stabilized. Initialization runs only once when the CAME method starts, and does not need to be repeated. This step could be completed when powering up the smartwatch.

When the magnet ring approaches ($d(t) = 1$), CAME recalculates the orientation of the smartwatch ($\mathbf{q}_t$) because biased magnetic field data might be fed into the AHRS. CAME saves IMU data and the reference ambient magnetic field ($^E\mathbf{B}_a(t)$) in a buffer. We termed this process "*rewind*" and the buffer as "*rewind buffer*." McIntosh et al. [33] originated this method. The size of the buffer is decided by evaluating the speed of a hand approaching a smartwatch. If the hand moves slowly, the buffer's size should be large because magnetic field data would biased for a long period. In contrast, if the user's hand moves fast, the buffer size can be small. In our case, the buffer size was set to 1.5 s.

Magnetic Field Distortion Detector

Numerous concepts for detecting distortion in the ambient magnetic field have been explored by various AHRS and HCI research projects. One method is to compare the magnitude of the magnetic field with a given threshold [33]. However, this is prone to error when the distribution of the ambient magnetic field is unstable. Moreover, the magnitude of the magnetic field may decrease even as the magnet ring approaches due to the directionality of the ambient magnetic field. In Figure 3, when oriented in the 6 o'clock direction, the magnitudes of the magnetic fields were more reduced with the magnet ring in place than it was not because the directionality of the fields were opposed and therefore canceled out the the ambient magnetic field.

Another approach is to use a dip angle [14, 48, 49]. A dip angle is the angle of intersection between gravity and the ambient magnetic field. Gravity is usually measured by an accelerometer. When a magnetic distortion occurs, the direction of the gravitational force does not change, but the direction of the magnetic field is affected instead. Therefore, a dip angle change may an indicate a magnetic distortion. This, however, does not apply to MagTouch. When a user raises a hand to use a smartwatch or swings hands when walking, an accelerometer measures gravitational force and linear acceleration. It is difficult to calculate an accurate dip angle under such conditions. In this study, we present the distortion detection method designed for MagTouch.

The distortion detector utilizes differences in the magnetic field vectors, not the differences in the magnitudes of the magnetic fields. In this way, it is possible to establish an index that is constantly increased by distortions of the the magnetic field. It is not reliable to directly use magnetometer data because it is affected by distortions of the magnetic field, but also by the rotation of the sensor relative to the earth. Therefore, CAME's distortion detector employs the measured magnetic field rotated to the earth reference frame ($^E\mathbf{B}_m(t)$). $^E\mathbf{B}_m(t)$ is stable in relatively close locations. If there is no distortion, $^E\mathbf{B}_m(t)$ does not change much no matter how the sensor moves. When a magnetic distortion happens, $^E\mathbf{B}_m(t)$ changes a lot because of the magnetic field around the smartwatch changes.

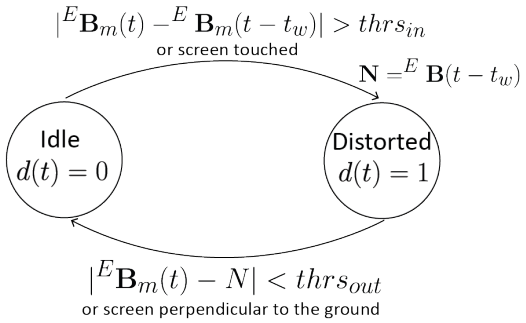

Figure 8. State diagram of the magnetic field distortion detector.

The distortion detector has two states, *Distorted* and *Idle* as the state diagram in Figure 8 illustrates. Each state indicates whether the ambient magnetic field is distorted or not. The detector changes its state to *Distorted* when $^E\mathbf{B}_m(t)$ changes more than the threshold ($thrs_{in}$) in specified period (t_w). To achieve this, the distortion detector requires a circular buffer. When the state switches to *Distorted*, the detector sets the magnetic field at the beginning of the buffer ($^E\mathbf{B}_m(t-t_w)$) as a reference. When the detector is in the *Distorted* state, it continuously compares the reference and the measured magnetic field. When the two vectors converge, the detector changes its state back to *Idle*. The size of the buffer (t_w) should be set based on the ambient magnetic field environment. If the ambient magnetic field is unstable, then the window size should be small enough not to produce false-positive errors. Moreover, the user's hand movement speed should be considered, as *rewind* process. In our case, the size of the buffer was set to 1.5 s.

Two additional state transition rules contributes to the distortion reliability. First, the detector reverts to the idle state when is no user interaction. The detector assumes that there is no user interaction when the side of the smartwatch faces down. Second, when the user taps the touchscreen, the state is changed to distort.

Machine Learning Classifier and Required Data

The machine learning of MagTouch system identifies a which finger is being used based on the estimated magnetic field of the magnet ring ($^S\mathbf{B}_r(t)$) and touch location data. MagTouch uses a support vector machine (SVM) for the machine-learning model. In our preliminary study, SVMs showed similar or better performance compared to other types of models, such as random forest or multi-layer perceptron. MagTouch uses SVM with the radial basis function (RBF) kernel. In the final design, LibSVM [8] was used for the machine learning model.

MagTouch requires training data drawn from various postures a smartwatch user might assume to handle changes of relative

position and orientation of the user's two hands. If data from only a specific posture were provided, the machine-learning model would be overfitted to that posture. We formulated various postures as illustrated in Figure 9. A user needs to collect machine-learning training data from these postures. The postures are formulated to vary numerous horizontal and vertical angles between a smartwatch and a hand. Posture A illustrates a comfortable position for the user rather than a specific one that the user should assume. The user must make an angle of 90° and 180° between the two arms in for postures B and C, respectively. For posture D, a user must to tilt the left arm inward, and vertically tap the touch screen. MagTouch uses a personalized model for each user because each user has a different finger length. Moreover, in our preliminary study, we observed that users have different behaviors when they tap a target on a smartwatch. For example, some users bent their fingers more than others did.

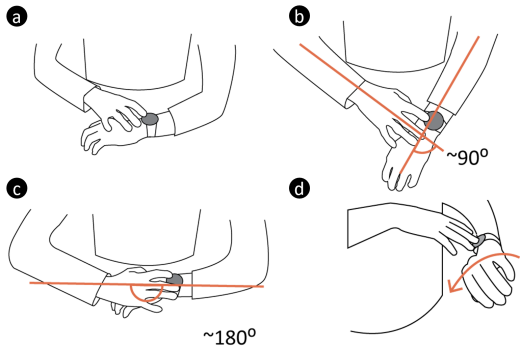

Figure 9. Training postures. a) A comfortable posture for a user. An angle between two arms is b) 90° and c) 180°. d) A posture that uses a smartwatch vertically by rotating the left arm inward.

Preliminary Evaluation of Magnetic Field Distortion Indexes

As mentioned earlier, various indexes can be used to measure the magnetic field distortion due to the magnet ring. The most popular ones are the magnitudes of the magnetic field and dip angles. CAME's distortion detector uses the difference of two ambient magnetic field vectors at the start and the end of its buffer ($|{}^{E}\mathbf{B}_m(t) - {}^{E}\mathbf{B}_m(t-t_w)|$). We will name this index as *the vector difference*. The indexes might have different characteristics. Therefore, as a preliminary evaluation, we tested the three indexes to see which one performed best with a simple threshold classifier. We considered various circumstances for using a smartwatch; such as wearing the watch, looking at the watch, walking with the watch and interacting with the watch. We measured the indexes for each situation and compared the accuracy of applying a simple threshold classifier to each index. Vector difference is the index for the *Idle* to *Distorted* transition. We could not test the index for the other state transition because that requires $thrs_{in}$ to be determined.

We recruited eight participants (one woman, mean age=26.8). Each participant proceeded with the following tasks. A participant stood up wearing the smartwatch. Targets appeared at random locations on the smartwatch for ten repetitions and the participant tapped the targets with the index finger. After each tap, the participant put his/her hands down. This task was repeated ten times. Next, the participant walked along the aisle for approximately 30 s, finally the participant unstrapped the smartwatch and put it on a desk.

For evaluation, we calculated F1-scores for different thresholds, to determine both false-positive and false-negative errors. Both errors might cause the erroneous reference ambient magnetic field. We devised a simple threshold classifier that classified a data point as *Distorted* if its value was larger than the threshold. We assumed data points 0.1 s before and after the taps as true *distorted* data points. We normalized all data by subtracting the mean, finding their absolute values, and scaling them from zero to one. An example is shown in Figure 11. We changed the threshold from zero to one and calculated the F1-scores.

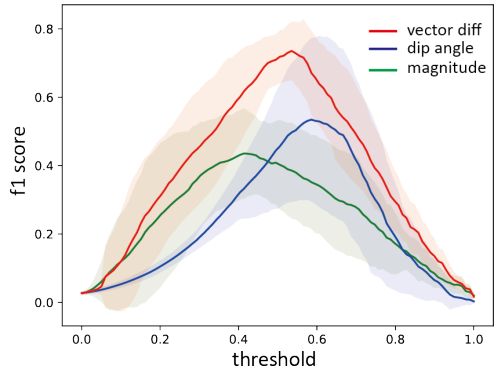

Figure 10. F1 scores of different indexes for the magnetic field distortion by different thresholds. Bold lines indicate mean values for different participants and the colored areas indicate the range of standard deviations.

In Figure 10, the CAME vector difference data shows the highest F1-score. It means when using a simple threshold classifier, it is appropriate to use the vector difference data for comparison to the other data. In the case of the dip angle data, it might cause false-positive errors when the motion of a smartwatch is accelerated. In Figure 11, for example, there are blue peaks that represent wearing the smartwatch, while raising a hand to check the watch and simply walking. The magnitude data, another index, is prone to errors in unstable distribution of the ambient magnetic field. There are high green peaks in the walking condition, where the ambient magnetic field value was unstable. Moreover, some magnitude data values were not as high as the other data for the tapping condition. This was due to different tapping positions. If the tapping position was far from the IMU sensor location, the magnitude value would be small. In comparison, the peak values of the vector difference data for the tapping condition were consistently high. This is because the magnitude of the difference between the two vectors is larger than the difference of the magnitude of two vectors ($|\mathbf{u}-\mathbf{v}| \geq |\mathbf{u}| - |\mathbf{v}|$). As an overall result of these factors, the vector difference data from CAME's magnetic distortion detector was the most appropriate data for the simple threshold classifier.

USER EVALUATION

The experiment consists of three parts, which were *Training*, followed by *Test 1* and *Test 2*. The training session collected

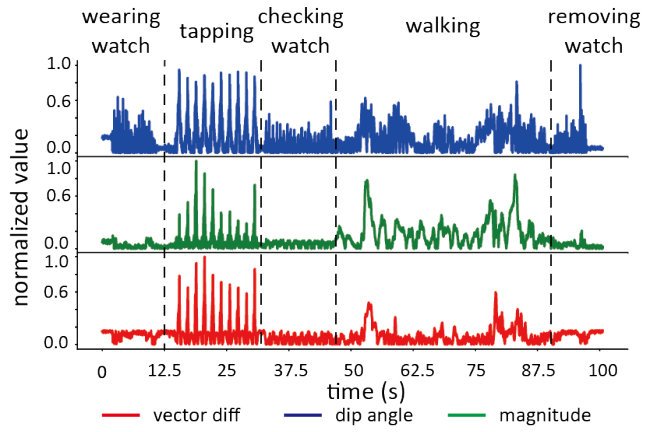

Figure 11. An example of different indexes for the magnetic field distortion detection.

data for the machine learning model. The two tests were real-time classification tests. Test 1 was for *multidirectional* evaluation. In this test, we investigated whether MagTouch can overcome directional changes in an ambient magnetic field. Test 2 was *in-context* evaluation. Test 2 measured accuracies in different postures in realistic usage contexts.

To understand the effectiveness of the CAME method, we compared classification accuracy results with raw magnetometer data (FingMag method [38]). In the case of the FingMag method, magnetometer measurements (${}^{S}\mathbf{B}_m(t)$) were used for the training and the testing, instead of the results of CAME (${}^{S}\mathbf{B}_r(t)$). Finger classifications for the FingMag method were done offline. We compare the results of the MagTouch and the FingMag methods in the Results section.

The participants removed any accessories on his/her hands and wrists before the training and the tests. We then asked the participants to tap a series of targets on the smartwatch to collect data. Furthermore, they removed the magnet ring and the smartwatch from their hands after each training and testing blocks. During the training and the tests, the MagTouch prototype logged the touch location data, the magnetic field data of the magnet ring (${}^{S}\mathbf{B}_r(t)$) and the raw magnetometer data for each tap.

Participants

We recruited 12 participants aged from 19 to 30 (mean age = 22.6, five male) via an online school community. All participants were right-handed. We measured the length of each participant's middle finger as the distance from the smartwatch and the magnet ring might affect classification accuracy. The average length of the middle fingers was 73.67 mm (SD = 3.42 mm)

Training MagTouch

There were eight blocks in the training session. For each block, a participant put on the smartwatch on the left wrist and wore the magnet ring on the right middle finger. Before wearing the smartwatch, a participant waited for 20 s for MagTouch's initialization step. After the participant wore the smartwatch

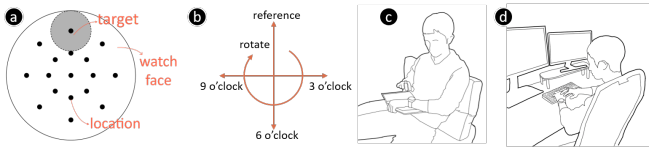

Figure 12. a) The smartwatch's diameter was 35mm (320 pixels), and the target's diameter was 11mm (100 pixels.) b) The four facing and rotational directions for Test 1. The reference direction was used in training. A participant c) reads a book and d) enters text using a keyboard for Test 2.

and the magnet ring, we asked the participant to stand up, and put his/her hands down for 5 to 10 seconds. The purpose of this procedure was to ensure that the magnetic field distortion detector was in the *Idle* state. Then, the participant started to tap targets on the smartwatch.

A training block consists of 102 targets (3 fingers $\times$ 17 positions $\times$ 2 repeats). The positions and the sizes of the targets are shown in Figure 12a. The order of the targets was randomized. As shown in Figure 9, there were four postures for the training session. A participant performed two training blocks for each posture. The order of the postures is the same as the order in Figure 9. As a result, a participant tapped 816 times (102 targets/block $\times$ 4 postures $\times$ 2 repeats). The participant faced the same direction for all the blocks. When a participant tapped a target with the wrong finger, we restarted that block.

Some participants intermittently tapped a target with the right side of his/her finger during the training blocks. Participants were instructed not to tap with the side of the finger. This instruction was also given in Test 1 and 2.

Experiments

Tasks

The objective of Test 1 was to assess how well MagTouch processes directional change in an ambient magnetic field. There were two types of tasks for Test 1. For the first task, a participant tapped targets while facing four different directions. These tasks were designed to test MagTouch in different stationary ambient magnetic fields. When a user faced a different direction, the direction of a magnetic field in the sensor frame changed. The four directions are shown in Figure 12b. For the second task, we asked a participant to rotate in place continuously while tapping targets. The objective of this task was to test MagTouch in a continuously changing ambient magnetic field. When a participant rotated, the ambient magnetic field that the smartwatch measured rotated as well. Test 1 was held in the same place as the training session, and the reference direction was the same as the participant had faced in the training session.

Test 2 measured recognition accuracies in different contexts. A smartwatch user's posture changes in different situations. For example, a usage posture is different when standing straight or when leaning back. We chose two common smartwatch usage contexts for this test. According to McMillan et al. [34], traveling, working, and relaxing were the most common activities when using a smartwatch. However, we excluded the traveling activities (e.g., walking, standing) because we surmised

that usage postures of such activities are similar to a standing condition. Finally, we created two usage contexts; one representing work and the other relaxation. The first is the typing context where the user types some text using a keyboard on a desk. The second is the reading context. A user leans back on a sofa and reads a book. Half of the participants completed the test for typing context first, and the other half completed reading context first.

Apparatus

Before testing began, a machine learning classifier was trained with each participant's data (touch data and ${}^{S}\mathbf{B}_r(t)$). We used a grid search method with 5–fold cross-validation to find appropriate C and γ of RBF kernels for each participant. The MagTouch prototype identified the contact fingers in real-time during the test sessions.

Procedure

Tests 1 and 2 were held on the day after the training session. Participants were instructed to adopt their individual comfortable-postures.

There were five blocks in Test 1. First four blocks were for the four directions in Figure 12b, and the last block was for the rotational movement. The four directions were the reference, 9 o'clock, 6 o'clock, and 3 o'clock. The procedure for every block duplicated the training session blocks except for the participants facing a different direction for each block. A participant tapped 510 (102 targets/block $\times$ (4 directions + 1 rotation)) targets for Test 1.

Test 2 was conducted immediately after Test 1 session. The second session consisted of two blocks, each corresponding a context. A participant executed the main task related to each context by reading a book while leaning back on a sofa or typing the consent form of this experiment on a desktop computer. The arrangements for each main task are shown in Figure 12c–d. Before beginning the main task, the participant waited until MagTouch is initialized. After putting on the smartwatch and the ring, participants placed their hands on their laps or on the desk for 5 to 10 seconds. The smartwatch emitted a short vibration which notified participants for the tapping task. Then, the participant tapped a segment of targets (10 to 12) as they had in Test 1. After tapping, the participant resumed the main task. The intervals between the segments were 30 to 60 seconds long. There were 10 segments in total, and the total number of targets was 153 (3 fingers $\times$ 17 positions $\times$ 3 repeats). The target order was randomized. Each participant tapped 306 targets in Test 2.

During the session, an experimenter manually checked if participants used the wrong finger and these were excluded from the analysis (three trials in Test 2). We found that one participant had a magnetic lipstick cap in her pocket and this affected the calibration. The participant restarted the test after the lipstick was removed.

Results

The average MagTouch accuracy result of Tests 1 and 2 was 95.03% ($SD = 3.22\%p$). Figure 13 shows the mean accuracies and standard deviations for Tests 1 and 2. The average FingMag accuracy result was 77.88% ($SD = 12.91\%p$).

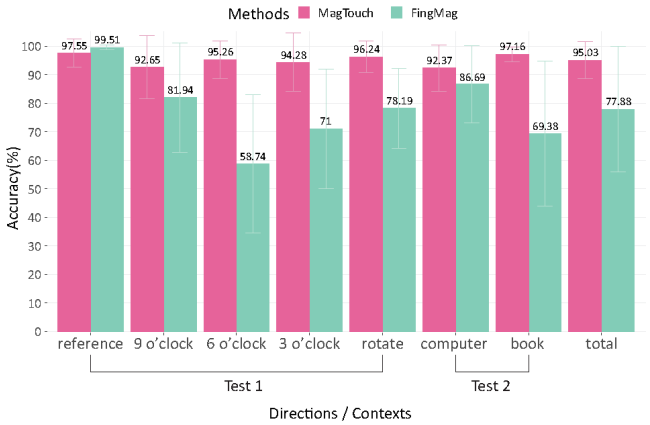

Figure 13. Mean accuracies for three-finger identification of Tests 1 and 2 in terms of the methods used. Error bars indicate standard deviations.

Figure 13 shows that the FingMag results for accuracy varied greatly depending on the participant's facing direction. The FingMag accuracy for the reference direction was high. However, it dropped when a user faced a different direction. Conversely, the MagTouch results for accuracy were all high ($> 90\%$) in all directions.

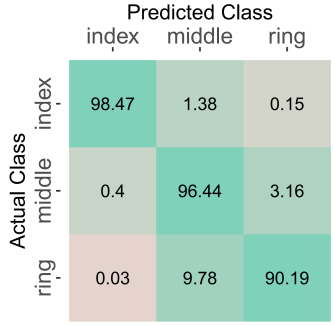

Figure 14. Confusion matrix of all the tests.

The confusion matrix (Figure 14) contains all data from the two tests. It shows that the middle and the ring finger were those most confused with each other.

We observed the participants' arm angles to understand how much various postures were used in the tests. We grouped participants into three categories based on their arm angles : small (90°–110°), medium (110°–150°), and large (150°–180°). Each participant could belong to more than one category because some participants changed posture during the tests. The results were (small = 2, medium = 8, large = 2) in Test 1, (small = 4, medium = 7, large = 2) in Test 2-reading, and (small=9, medium=5, large=0) in Test 2-typing. These results demonstrate that our tests led participants to adopt a variety of postures. The reason for many participants adopting small-angle postures in Test 2-typing was they often kept stayed their left hands on the keyboard while tapping on the watch.

DISCUSSION

The average recognition accuracy for MagTouch was 95.03%, which is a 22% improvement over the FingMag results. The MagTouch recognition accuracy was consistently high, thereby demonstrating the efficacy of cancelling the effects of an ambient magnetic field. Conversely, FingMag's recognition accuracy dropped significantly when the participant faced a direction during the test different to that when training. Test 2 also displayed reliable recognition performance in contexts involving different postures and when being close to electronic devices that caused magnetic field interference.

Most finger confusion was observed to occur between the middle finger and the ring finger. Based on participants' feedback and our observations, we conjecture that the participants' posture had an effect on the classification error. Some participants reported that it was uncomfortable to tap with a ring finger, and we noted that participants rotated the ringed hand because a large part of the screen was occluded. Owing to the discomfort and the occlusion, the participants might have tried various postures to find the optimal position. This may indicate the need to consider collecting more data for the ring finger than the others.

We compared our results with TriTap, where they also classified the three fingers as we did, but only used the touchscreen of a smartwatch. MagTouch demonstrated an accuracy 16% higher than the TriTap's accuracy (79.4%) for the natural tapping condition. Moreover, TriTap was only tested in a situation with participants resting their arms on a desk. In contrast, MagTouch was also tested in different contexts.

The increased input vocabulary can be used as shortcuts or chords as demonstrated in previous research, but we also believe that it can be helpful for entering short text or number phrases, such as PIN codes. Many smartwatches input 4-digit or 6-digit PINs using keypads. It is possible to increase the number of combinations with MagTouch while reducing the number of keystrokes. For example, 4-digit 10-key PINs have up to 10,000 combinations, but 3-digit 10-key PINs with MagTouch have 27,000 combinations, 2.7 times more while reducing the number of keystrokes by 25%.

LIMITATION AND FUTURE WORK

While the experiment showed very promising results, there are two possible cases where MagTouch could make an error by inaccurately sampling an ambient magnetic field. The first case is when the user has magnetic material in her pocket. In this case, the distortion detector is in the idle state and MagTouch samples the magnetic field around the pocket as the reference ambient magnetic field (${}^{E}\mathbf{B}_a(t)$). When the user taps the smartwatch, the rewind process runs, and the magnetic field around the pocket is stored for use as the ${}^{E}\mathbf{B}_a(t)$. In such cases, we think it is possible to warn the user that MagTouch might need recalibration. Just as map applications warn users when a digital compass needs recalibration. MagTouch could sense a nearby magnet if a substantial magnetometer value is detected when a user is not interacting with the smartwatch. It can then inform the user that MagTouch might have to resample the correct ambient magnetic field.

The second case is when MagTouch is used within a highly distorted magnetic field, for example, walking beside a large metal wall. The MagTouch method doesn't take account of variations of the ambient magnetic field when it is in the *Distorted* state. However, MagTouch can manage some variations. In the rotating test in Test 1, the difference in the ambient magnetic field was up to 10 μT, when a participant rotated while using the smartwatch. The 10 μT variation is not smaller than that caused by other buildings [21, 43]. Nonetheless, further study is needed to establish the common variation of magnetic field levels.

Another limitation is that the training process may be burdensome for some users. Fortunately, it might be possible to omit the training process altogether. Let us say a user uses MagTouch with a general classifier, which being a classifier trained with different people's data. It would then collect unlabeled data during use. With this data, it might be possible to personalize the general classifier with semi-supervised learning techniques. We tested a general classifier with the data we collected throughout the tests, and it scored a 92.64% ($SD = 9.25\% p$) match. We think this is acceptable for initial accuracy. Another straightforward solution is to collect a small amount of data during multiple sessions over an extended period (e.g. few days), rather than all at once. During the training period, the general classifier could be applied until all the required data is collected.

The magnetic field distortion detector that we designed for MagTouch could be applied to other projects. Magnetic field anomaly detection has been studied in the HCI field [33, 49], and in AHRS research projects [14, 25, 48]. Our distortion detector could be used for present and future HCI research that uses magnets, and AHRS systems to adapt to magnetic field disturbances. We will explore how the distortion detector can enhance existing systems.

We believe that MagTouch can be applied to other devices with touch sensors and IMUs as well, such as smartphones and smart glasses. The increased touch input vocabulary will enhance users' experience by enabling rapid microinteractions on these devices and by minimizing the distractions caused by such interactions.

CONCLUSION

This paper introduced MagTouch; a robust and practical finger identification method that uses magnetic field data and touch location. MagTouch uses a magnet ring that does not require any external power and is less disruptive to daily activities than fingertip magnets. The paper proposes solutions, such as the algorithm to eliminate the effects of the ambient magnetic field, to solve problems caused by having a magnet at a distance from the smartwatch. Our evaluation revealed that the system could identify the three fingers used for smartwatch interactions at a 95.03% accuracy rate.

ACKNOWLEDGMENTS

This research was supported by Next-Generation Information Computing Development Program through the National Research Foundation of Korea(NRF) funded by the Ministry of Science, ICT (2017M3C4A7065963).

REFERENCES

[1] Daniel Ashbrook, Patrick Baudisch, and Sean White. 2011. Nenya: Subtle and Eyes-free Mobile Input with a Magnetically-tracked Finger Ring. In *Proceedings of the SIGCHI Conference on Human Factors in Computing Systems (CHI '11)*. ACM, New York, NY, USA, 2043–2046. DOI: http://dx.doi.org/10.1145/1978942.1979238

[2] Daniel L. Ashbrook. 2010. *Enabling Mobile Microinteractions*. Ph.D. Dissertation. Atlanta, GA, USA. Advisor(s) Starner, Thad E. AAI3414437.

[3] Daniel L. Ashbrook, James R. Clawson, Kent Lyons, Thad E. Starner, and Nirmal Patel. 2008. Quickdraw: The Impact of Mobility and On-body Placement on Device Access Time. In *Proceedings of the SIGCHI Conference on Human Factors in Computing Systems (CHI '08)*. ACM, New York, NY, USA, 219–222. DOI: http://dx.doi.org/10.1145/1357054.1357092

[4] Halim Cagri Ates, Ilias Apostolopoulos, and Eelke Folmer. 2015. Expanding the Vocabulary of Multitouch Input using Magnetic Fingerprints. *CoRR* abs/1501.03218 (2015). http://arxiv.org/abs/1501.03218

[5] Oscar Kin-Chung Au and Chiew-Lan Tai. 2010. Multitouch Finger Registration and Its Applications. In *Proceedings of the 22Nd Conference of the Computer-Human Interaction Special Interest Group of Australia on Computer-Human Interaction (OZCHI '10)*. ACM, New York, NY, USA, 41–48. DOI: http://dx.doi.org/10.1145/1952222.1952233

[6] Allison A. Bailey and Peter L. Hurd. 2005. Finger length ratio (2D:4D) correlates with physical aggression in men but not in women. *Biological Psychology* 68, 3 (2005), 215 – 222. DOI:http://dx.doi.org/https://doi.org/10.1016/j.biopsycho.2004.05.001

[7] Hrvoje Benko, T. Scott Saponas, Dan Morris, and Desney Tan. 2009. Enhancing Input on and Above the Interactive Surface with Muscle Sensing. In *Proceedings of the ACM International Conference on Interactive Tabletops and Surfaces (ITS '09)*. ACM, New York, NY, USA, 93–100. DOI: http://dx.doi.org/10.1145/1731903.1731924

[8] Chih-Chung Chang and Chih-Jen Lin. 2011. LIBSVM: A Library for Support Vector Machines. *ACM Trans. Intell. Syst. Technol.* 2, 3, Article 27 (May 2011), 27 pages. DOI:http://dx.doi.org/10.1145/1961189.1961199

[9] Ke-Yu Chen, Kent Lyons, Sean White, and Shwetak Patel. 2013. uTrack: 3D Input Using Two Magnetic Sensors. In *Proceedings of the 26th Annual ACM Symposium on User Interface Software and Technology (UIST '13)*. ACM, New York, NY, USA, 237–244. DOI: http://dx.doi.org/10.1145/2501988.2502035

[10] Ke-Yu Chen, Shwetak N. Patel, and Sean Keller. 2016. Finexus: Tracking Precise Motions of Multiple Fingertips Using Magnetic Sensing. In *Proceedings of the 2016 CHI Conference on Human Factors in Computing Systems (CHI '16)*. ACM, New York, NY, USA, 1504–1514. DOI: http://dx.doi.org/10.1145/2858036.2858125

[11] Victor Cheung and Audrey Girouard. 2018. Exploring Around-Device Tangible Interactions for Mobile Devices with a Magnetic Ring. In *Proceedings of the Twelfth International Conference on Tangible, Embedded, and Embodied Interaction (TEI '18)*. ACM, New York, NY, USA, 108–114. DOI: http://dx.doi.org/10.1145/3173225.3173283

[12] Ashley Colley and Jonna Häkkilä. 2014. Exploring Finger Specific Touch Screen Interaction for Mobile Phone User Interfaces. In *Proceedings of the 26th Australian Computer-Human Interaction Conference on Designing Futures: The Future of Design (OzCHI '14)*. ACM, New York, NY, USA, 539–548. DOI: http://dx.doi.org/10.1145/2686612.2686699

[13] Philipp Ewerling, Alexander Kulik, and Bernd Froehlich. 2012. Finger and Hand Detection for Multi-touch Interfaces Based on Maximally Stable Extremal Regions. In *Proceedings of the 2012 ACM International Conference on Interactive Tabletops and Surfaces (ITS '12)*. ACM, New York, NY, USA, 173–182. DOI: http://dx.doi.org/10.1145/2396636.2396663

[14] Bingfei Fan, Qingguo Li, Chao Wang, and Tao Liu. 2017. An Adaptive Orientation Estimation Method for Magnetic and Inertial Sensors in the Presence of Magnetic Disturbances. *Sensors* 17, 5 (2017). DOI: http://dx.doi.org/10.3390/s17051161

[15] Hyunjae Gil, DoYoung Lee, Seunggyu Im, and Ian Oakley. 2017. TriTap: Identifying Finger Touches on Smartwatches. In *Proceedings of the 2017 CHI Conference on Human Factors in Computing Systems (CHI '17)*. ACM, New York, NY, USA, 3879–3890. DOI:http://dx.doi.org/10.1145/3025453.3025561

[16] Alix Goguey, Géry Casiez, Daniel Vogel, Fanny Chevalier, Thomas Pietrzak, and Nicolas Roussel. 2014. A Three-step Interaction Pattern for Improving Discoverability in Finger Identification Techniques. In *Proceedings of the Adjunct Publication of the 27th Annual ACM Symposium on User Interface Software and Technology (UIST'14 Adjunct)*. ACM, New York, NY, USA, 33–34. DOI: http://dx.doi.org/10.1145/2658779.2659100

[17] Aakar Gupta, Muhammed Anwar, and Ravin Balakrishnan. 2016. Porous Interfaces for Small Screen Multitasking Using Finger Identification. In *Proceedings of the 29th Annual Symposium on User Interface Software and Technology (UIST '16)*. ACM, New York, NY, USA, 145–156. DOI: http://dx.doi.org/10.1145/2984511.2984557

[18] Aakar Gupta and Ravin Balakrishnan. 2016. DualKey: Miniature Screen Text Entry via Finger Identification. In *Proceedings of the 2016 CHI Conference on Human Factors in Computing Systems (CHI '16)*. ACM, New York, NY, USA, 59–70. DOI: http://dx.doi.org/10.1145/2858036.2858052

[19] Xinying Han, Hiroaki Seki, Yoshitsugu Kamiya, and Masatoshi Hikizu. 2007. Wearable handwriting input device using magnetic field. In *SICE Annual Conference 2007*. 365–368. DOI: http://dx.doi.org/10.1109/SICE.2007.4421009

[20] Chris Harrison and Scott E. Hudson. 2009. Abracadabra: Wireless, High-precision, and Unpowered Finger Input for Very Small Mobile Devices. In *Proceedings of the 22Nd Annual ACM Symposium on User Interface Software and Technology (UIST '09)*. ACM, New York, NY, USA, 121–124. DOI: http://dx.doi.org/10.1145/1622176.1622199

[21] Janne Haverinen and Anssi Kemppainen. 2009. Global indoor self-localization based on the ambient magnetic field. *Robotics and Autonomous Systems* 57, 10 (2009), 1028–1035.

[22] Christian Holz and Patrick Baudisch. 2013. Fiberio: A Touchscreen That Senses Fingerprints. In *Proceedings of the 26th Annual ACM Symposium on User Interface Software and Technology (UIST '13)*. ACM, New York, NY, USA, 41–50. DOI: http://dx.doi.org/10.1145/2501988.2502021

[23] Azusa Kadomura and Itiro Siio. 2015. MagNail: User Interaction with Smart Device Through Magnet Attached to Fingernail. In *Adjunct Proceedings of the 2015 ACM International Joint Conference on Pervasive and Ubiquitous Computing and Proceedings of the 2015 ACM International Symposium on Wearable Computers (UbiComp/ISWC'15 Adjunct)*. ACM, New York, NY, USA, 309–312. DOI: http://dx.doi.org/10.1145/2800835.2800859

[24] Hamed Ketabdar, Mehran Roshandel, and Kamer Ali Yüksel. 2010. Towards Using Embedded Magnetic Field Sensor for Around Mobile Device 3D Interaction. In *Proceedings of the 12th International Conference on Human Computer Interaction with Mobile Devices and Services (MobileHCI '10)*. ACM, New York, NY, USA, 153–156. DOI: http://dx.doi.org/10.1145/1851600.1851626

[25] J. Lee, J. Lim, and J. Lee. 2018. Compensated Heading Angles for Outdoor Mobile Robots in Magnetically Disturbed Environment. *IEEE Transactions on Industrial Electronics* 65, 2 (Feb 2018), 1408–1419. DOI:http://dx.doi.org/10.1109/TIE.2017.2726958

[26] Rong-Hao Liang, Kai-Yin Cheng, Liwei Chan, Chuan-Xhyuan Peng, Mike Y. Chen, Rung-Huei Liang, De-Nian Yang, and Bing-Yu Chen. 2013. GaussBits: Magnetic Tangible Bits for Portable and Occlusion-free Near-surface Interactions. In *Proceedings of the SIGCHI Conference on Human Factors in Computing Systems (CHI '13)*. ACM, New York, NY, USA, 1391–1400. DOI:http://dx.doi.org/10.1145/2470654.2466185

[27] Xin Liu, Katia Vega, Pattie Maes, and Joe A. Paradiso. 2016. Wearability Factors for Skin Interfaces. In *Proceedings of the 7th Augmented Human International Conference 2016 (AH '16)*. ACM, New York, NY, USA, Article 21, 8 pages. DOI: http://dx.doi.org/10.1145/2875194.2875248

[28] S. O. H. Madgwick, A. J. L. Harrison, and R. Vaidyanathan. 2011. Estimation of IMU and MARG orientation using a gradient descent algorithm. In *2011 IEEE International Conference on Rehabilitation Robotics*. 1–7. DOI: http://dx.doi.org/10.1109/ICORR.2011.5975346

[29] Nicolai Marquardt, Johannes Kiemer, and Saul Greenberg. 2010. What Caused That Touch?: Expressive Interaction with a Surface Through Fiduciary-tagged Gloves. In *ACM International Conference on Interactive Tabletops and Surfaces (ITS '10)*. ACM, New York, NY, USA, 139–142. DOI: http://dx.doi.org/10.1145/1936652.1936680

[30] Nicolai Marquardt, Johannes Kiemer, David Ledo, Sebastian Boring, and Saul Greenberg. 2011. Designing User-, Hand-, and Handpart-aware Tabletop Interactions with the TouchID Toolkit. In *Proceedings of the ACM International Conference on Interactive Tabletops and Surfaces (ITS '11)*. ACM, New York, NY, USA, 21–30. DOI:http://dx.doi.org/10.1145/2076354.2076358

[31] Damien Masson, Alix Goguey, Sylvain Malacria, and Géry Casiez. 2017. WhichFingers: Identifying Fingers on Touch Surfaces and Keyboards Using Vibration Sensors. In *Proceedings of the 30th Annual ACM Symposium on User Interface Software and Technology (UIST '17)*. ACM, New York, NY, USA, 41–48. DOI: http://dx.doi.org/10.1145/3126594.3126619

[32] J. McCann, R. Hurford, and A. Martin. 2005. A design process for the development of innovative smart clothing that addresses end-user needs from technical, functional, aesthetic and cultural view points. In *Ninth IEEE International Symposium on Wearable Computers (ISWC'05)*. 70–77. DOI: http://dx.doi.org/10.1109/ISWC.2005.3

[33] Jess McIntosh, Paul Strohmeier, Jarrod Knibbe, Sebastian Boring, and Kasper Hornbæk. 2019. Magnetips: Combining Fingertip Tracking and Haptic Feedback for Around-Device Interaction. In *Proceedings of the 2019 CHI Conference on Human Factors in Computing Systems (CHI '19)*. ACM, New York, NY, USA, Article 408, 12 pages. DOI: http://dx.doi.org/10.1145/3290605.3300638

[34] Donald McMillan, Barry Brown, Airi Lampinen, Moira McGregor, Eve Hoggan, and Stefania Pizza. 2017. Situating Wearables: Smartwatch Use in Context. In *Proceedings of the 2017 CHI Conference on Human Factors in Computing Systems (CHI '17)*. ACM, New York, NY, USA, 3582–3594. DOI: http://dx.doi.org/10.1145/3025453.3025993

[35] Sundar Murugappan, Vinayak, Niklas Elmqvist, and Karthik Ramani. 2012. Extended Multitouch: Recovering Touch Posture and Differentiating Users Using a Depth Camera. In *Proceedings of the 25th*

Annual ACM Symposium on User Interface Software and Technology (UIST '12). ACM, New York, NY, USA, 487–496. DOI: http://dx.doi.org/10.1145/2380116.2380177

[36] Jeyaseelan Nadankutty, Norashikin Mohd Shaharuddin, Phavitra Jeyabalan, Rodney Arnold, Lourdes Thomas, Thasha Thiruselvam, and Yasini Ramaiah. 2014. Digit ratio, 2D: 4D (Index finger: Ring finger) in the right and left hand of males and females in Malaysia. *Open Science Repository Anthropology* open-access (2014), e45011806.

[37] Antti Oulasvirta, Sakari Tamminen, Virpi Roto, and Jaana Kuorelahti. 2005. Interaction in 4-second Bursts: The Fragmented Nature of Attentional Resources in Mobile HCI. In *Proceedings of the SIGCHI Conference on Human Factors in Computing Systems (CHI '05)*. ACM, New York, NY, USA, 919–928. DOI: http://dx.doi.org/10.1145/1054972.1055101

[38] Keunwoo Park and Geehyuk Lee. 2019. FingMag: Finger Identification Method for Smartwatch. In *Extended Abstracts of the 2019 CHI Conference on Human Factors in Computing Systems (CHI EA '19)*. ACM, New York, NY, USA, Article LBW2216, 6 pages. DOI:http://dx.doi.org/10.1145/3290607.3312982

[39] Michael Peters, Kevin Mackenzie, and Pam Bryden. 2002. Finger length and distal finger extent patterns in humans. *American Journal of Physical Anthropology: The Official Publication of the American Association of Physical Anthropologists* 117, 3 (2002), 209–217.

[40] Stefania Pizza, Barry Brown, Donald McMillan, and Airi Lampinen. 2016. Smartwatch in Vivo. In *Proceedings of the 2016 CHI Conference on Human Factors in Computing Systems (CHI '16)*. ACM, New York, NY, USA, 5456–5469. DOI: http://dx.doi.org/10.1145/2858036.2858522

[41] Julie Rico and Stephen Brewster. 2010. Gesture and Voice Prototyping for Early Evaluations of Social Acceptability in Multimodal Interfaces. In *International Conference on Multimodal Interfaces and the Workshop on Machine Learning for Multimodal Interaction (ICMI-MLMI '10)*. ACM, New York, NY, USA, Article 16, 9 pages. DOI: http://dx.doi.org/10.1145/1891903.1891925

[42] Quentin Roy, Yves Guiard, Gilles Bailly, Éric Lecolinet, and Olivier Rioul. 2015. Glass+Skin: An Empirical Evaluation of the Added Value of Finger Identification to Basic Single-Touch Interaction on Touch Screens. In *Human-Computer Interaction – INTERACT 2015*, Julio Abascal, Simone Barbosa, Mirko Fetter, Tom Gross, Philippe Palanque, and Marco Winckler (Eds.). Springer International Publishing, Cham, 55–71.

[43] A. Solin, M. Kok, N. Wahlström, T. B. Schön, and S. Särkkä. 2018. Modeling and Interpolation of the Ambient Magnetic Field by Gaussian Processes. *IEEE Transactions on Robotics* 34, 4 (Aug 2018), 1112–1127. DOI:http://dx.doi.org/10.1109/TRO.2018.2830326

[44] Srinath Sridhar, Anders Markussen, Antti Oulasvirta, Christian Theobalt, and Sebastian Boring. 2017. WatchSense: On- and Above-Skin Input Sensing Through a Wearable Depth Sensor. In *Proceedings of the 2017 CHI Conference on Human Factors in Computing Systems (CHI '17)*. ACM, New York, NY, USA, 3891–3902. DOI: http://dx.doi.org/10.1145/3025453.3026005

[45] Atsushi Sugiura and Yoshiyuki Koseki. 1998. A User Interface Using Fingerprint Recognition: Holding Commands and Data Objects on Fingers. In *Proceedings of the 11th Annual ACM Symposium on User Interface Software and Technology (UIST '98)*. ACM, New York, NY, USA, 71–79. DOI: http://dx.doi.org/10.1145/288392.288575

[46] Julie Wagner, Eric Lecolinet, and Ted Selker. 2014. Multi-finger Chords for Hand-held Tablets: Recognizable and Memorable. In *Proceedings of the SIGCHI Conference on Human Factors in Computing Systems (CHI '14)*. ACM, New York, NY, USA, 2883–2892. DOI: http://dx.doi.org/10.1145/2556288.2556958

[47] Jingtao Wang and John Canny. 2004. FingerSense: Augmenting Expressiveness to Physical Pushing Button by Fingertip Identification. In *CHI '04 Extended Abstracts on Human Factors in Computing Systems (CHI EA '04)*. ACM, New York, NY, USA, 1267–1270. DOI:http://dx.doi.org/10.1145/985921.986040

[48] Nagesh Yadav and Chris Bleakley. 2014. Accurate Orientation Estimation Using AHRS under Conditions of Magnetic Distortion. *Sensors* 14, 11 (2014), 20008–20024. DOI: http://dx.doi.org/10.3390/s141120008

[49] Sang Ho Yoon, Yunbo Zhang, Ke Huo, and Karthik Ramani. 2016. TRing: Instant and Customizable Interactions with Objects Using an Embedded Magnet and a Finger-Worn Device. In *Proceedings of the 29th Annual Symposium on User Interface Software and Technology (UIST '16)*. ACM, New York, NY, USA, 169–181. DOI: http://dx.doi.org/10.1145/2984511.2984529

[50] Jingjie Zheng and Daniel Vogel. 2016. Finger-Aware Shortcuts. In *Proceedings of the 2016 CHI Conference on Human Factors in Computing Systems (CHI '16)*. ACM, New York, NY, USA, 4274–4285. DOI: http://dx.doi.org/10.1145/2858036.2858355